PERGAMON

Journal of Quantitative Spectroscopy & Radiative Transfer 81 (2003) 421–429

Journal of Quantitative Spectroscopy & Radiative Transfer

www.elsevier.com/locate/jqsrt

Hard X-ray emission from laser-produced plasmas of U and Pb recorded by a transmission crystal spectrometer

J.F. Seely[a,*], R. Doron[b], A. Bar-Shalom[c], L.T. Hudson[d], C. Stoeckl[e]

[a] *Naval Research Laboratory, Space Science Division, Washington, DC 20375, USA*
[b] *School of Computational Sciences, George Mason University, Fairfax, VA 22030, USA*
[c] *ARTEP Inc., Columbia, MD 21045, USA*
[d] *National Institute of Standards and Technology, Gaithersburg, MD 20899, USA*
[e] *Laboratory for Laser Energetics, University of Rochester, Rochester, NY 14623, USA*

Accepted 15 February 2003

Abstract

Hard X-ray spectra from laser-produced plasmas were recorded by a transmission crystal survey spectrometer covering the 12–60 keV energy range with a resolving power of $E/\Delta E \cong 100$. This emission is of interest for the development of hard X-ray backlighters and hot electron diagnostics. Foils of U and Pb were irradiated at the OMEGA laser facility by 24 beams (12 on each side), each with an energy of ≅500 J, a pulse duration of 1 ns, and no beam smoothing. The beams were focused to a 50 μm diameter spot on the target plane. The spectra typically exhibit a few intense and relatively narrow features in the 12–22 keV energy range. Initial analysis suggests that these hard X-ray features are inner-shell transitions resulting from L-shell vacancies created by energetic electrons. The observed transition energies are slightly higher than the neutral-atom characteristic X-ray energies. Calculations suggest that the transitions are in the Ni-like or lower ionization stages. The analysis further indicates that opacity effects play an important role in producing the spectra.
Published by Elsevier Science Ltd.

Keywords: X-ray spectroscopy; Plasma spectroscopy; Highly charged ions

1. Introduction

A hard X-ray spectrometer (HXS) covering the 12–60 keV energy range was fielded at the OMEGA laser. The spectra from U and Pb targets were dispersed by a cylindrically bent quartz (10–11) transmission crystal, and the time-integrated spectral images were recorded by a CCD detector. This is the first use of a transmission (Laué) crystal to record the spectra of high atomic number

* Corresponding author. Tel.: +1-202-767-3529; fax: +1-202-404-7997.
E-mail address: john.seely@nrl.navy.mil (J.F. Seely).

0022-4073/03/$ - see front matter. Published by Elsevier Science Ltd.
doi:10.1016/S0022-4073(03)00092-X

elements in hot and dense laser-produced plasmas. The advantages of utilizing a cylindrically bent transmission crystal for this application are the wide energy coverage, the compact and linear optical system that is compatible with instrument insertion modules, and focusing through a slit that facilitates hard X-ray and energetic particle shielding.

The details of the instrument design and performance as well as, for example, spectral images recorded from CH, Kr, and Ag targets were presented in Ref. [1]. In this paper, we report the recording of spectra emitted from the much higher Z targets of U and Pb planar foils. In Section 2 we briefly describe the spectrometer and the experimental setup at the OMEGA facility. In Section 3 we describe the obtained spectra and give a preliminary analysis. A summary is given in Section 4.

2. Instrument design

As shown in Fig. 1, the spectrometer is composed of an entrance aperture plane at the front of the instrument, a cylindrically bent crystal, scatter shielding, and a charge coupled device (CCD) detector with 1360 rows and 1840 columns of pixels. X rays are dispersed by the crystal in transmission geometry, pass through a polychromatic focal slit, and are recorded by the planar detector that intersects the focusing circle whose diameter equals the radius of curvature of the crystal (112 mm). The quartz crystal was aligned, cut, and mounted such that the 10–11 planes (3.34 Å lattice spacing) are perpendicular to the plane of dispersion.

As shown in Fig. 2, the instrument produces two spectral representations that are registered on the detector as mirror images of one another. The two spectra are ideally symmetric about the central axis of the instrument. A pinhole is present in the entrance aperture plane, and a pinhole image of the X-ray source appears at the center of the spectral image.

Various metal filters needed for calibrating the energy scale are positioned along the polychromatic focal slit. This results in a number of filtered regions in the direction perpendicular to the dispersion plane as seen in the spectral image of Fig. 2. The central part of the slit and the spectral image are unfiltered. A blast-shield filter (137 μm Be) was positioned in the instrument's nosecone. An additional filter covered the pinhole and provided an independent means of adjusting the attenuation of the intense pinhole image. Lead shielding (1.3 cm thick) at the entrance aperture plane and

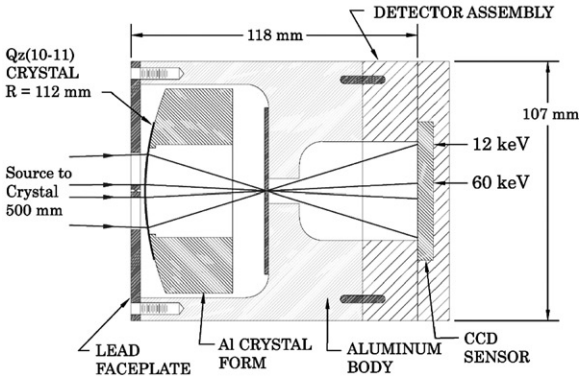

Fig. 1. Optical layout of the X-ray spectrometer.

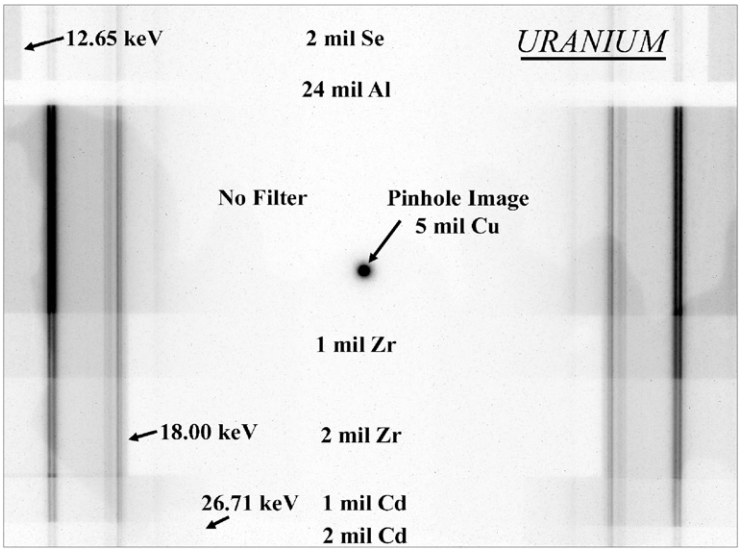

Fig. 2. The spectral image acquired from the uranium foil target. The filter regions and the edge energies are indicated.

on either side of the polychromatic focusing slit prevented undispersed hard X-rays from directly reaching the CCD detector.

For the U and Pb spectra presented here, the pinhole filter was 127 μm Cu. A 51 μm Se filter was positioned at the top of the polychromatic focal slit, and the attenuation by the filter's 610 μm aluminum frame also appears near the top of the spectral image (see Fig. 2). Zr and Cd filters, each 25 and 51 μm thick, were positioned at the bottom of the slit. The center of the slit had no filter.

The U and Pb targets were planar foils and were 25 μm thick. The targets were irradiated by 12 OMEGA beams on each side of the foils (total of 24 beams) with a range of incidence angles. The beams incident on each side of the foil were overlapping with an approximately 50 μm focal spot diameter. Each beam had a 1 ns square pulse, and no beam smoothing was applied. The total incident laser energy was typically 11.6 kJ.

The instrument axis was aligned to the laser focal spot using a mechanical pointer, and the target plane was perpendicular to the instrument axis. This alignment resulted in symmetric illumination of the crystal. The target to crystal distance was 50 cm.

The X-ray energy scale was initially established by utilizing the characteristic X-ray lines from a laboratory source. However, owing to the possible small misalignment of the instrument axis to the laser focal spot in the dispersion direction, the energy scale may slightly differ from that determined in the laboratory. The filter edges appearing in the U and Pb spectral images were used to make in situ adjustments to the energy scale. The energy scale was modeled by an analytical equation that was based on the geometry of the spectrometer: $E^2 = a + b/(x - x_0)^2 + c/(x - x_0)$ where x is the pixel position in the dispersion direction, and x_0 is the pixel position of the center of the spectral image. Ideally, x_0 is at the center of the CCD and the center of the pinhole image, and the first two terms in the energy scale equation exactly fit the observed positions of the filter edges [1]. The last term in the energy scale equation, $c/(x - x_0)$, empirically accounts for the non-ideal focusing of the

spectral image and pointing of the instrument axis. The parameters a, b, c, and x_0 were derived from the filter edges observed in each spectral image using a least-squares fitting technique. The assumed reference energies were from Ref. [2]: Se (12.65 keV), Zr (18.00 keV), and Cd (26.71 keV). Thus six edge energies (three on each side of the spectral image) were used to determine four fitting parameters (a, b, c, and x_0). The average difference between the calculated edge energies and the reference values was 95 eV, and this represents the accuracy of the energy scale. The accuracy of the energy scale (95 eV) depends on the spectral resolving power ($\sim$100), the X-ray continuum exposure levels at the edge positions, the number of filter edges observed, and the accuracy of the energy scale equation.

3. Uranium and lead spectra

The central region of the U spectral image, with no filter as shown in Fig. 2, was summed in the vertical direction (perpendicular to the dispersion plane). The resulting spectrum from the right side of the spectral image, which has better exposure and resolution than the left side, is shown in Fig. 3. The corresponding spectrum from the Pb target is also shown in Fig. 3. The energies of the spectral features marked by the numbers in Fig. 3 are listed in Table 1.

The measured energies were initially compared to the energies of the characteristic (neutral atom) L X-ray transitions from Ref. [3] and listed in Table 2. The strongest characteristic U spectral features are expected to be the Lα_1 and Lα_2 doublet with energies 13.6147 and 13.4388 keV, respectively. These are transitions of the type $2p_{3/2}$–$3d_{5/2}$ and $2p_{3/2}$–$3d_{3/2}$, respectively. From Table 1, the observed energies of the two most intense features in the U spectrum (numbers 2 and 1) are 13.87 and 13.67 keV. The observed energies are 260 and 230 eV higher than the Lα_1 and Lα_2 energies, respectively. These differences exceed the 95 eV uncertainty of the energy scale.

The next most intense uranium characteristic X-ray transition is the Lβ_1 $2p_{1/2}$–$3d_{3/2}$ transition at 17.2200 keV. A relatively intense feature is observed at 17.28 keV (number 6 in Fig. 3 and Table 1), 60 eV higher than the Lβ_1 transition. This energy difference is smaller than the estimated uncertainty of the experimental energy scale (95 eV).

As seen in Fig. 3 and Table 2, the Pb Lα_1 and Lα_2 characteristic transitions at 10.5515 and 10.4495 keV were beyond the range of observation. The energy region of the Lβ_1 transition (12.6137 keV) was observed. Intense spectral features were observed at 12.70 and 12.87 keV (numbers 1 and 2 in Fig. 3 and Table 1), 90 and 260 eV higher than the Lβ_1 energy. These energy differences are comparable to or higher than the 95 eV uncertainty of the experimental energy scale.

Since the most intense observed U and Pb spectral features appear to have energies that are higher than the characteristic neutral-atom transitions, it is plausible that the observed transitions are in highly-charged ions. In order to investigate this possibility, in a first step the energies of the L-shell transitions in the closed shell ions Ne-, Ar-, and Ni-like were calculated. These calculations were later extended to include also the lower charge states of Cu- and Zn-like uranium. The calculations were performed using the HULLAC code [4], which is most suitable for calculating the atomic properties of such highly-ionized heavy ions. The accuracy of the calculated energies of transitions with $\Delta n \geqslant 1$ (where n is the principal quantum number) is generally expected to be better than 1%. In particular, for the special cases of highly charged ions with a closed shell or with only a few electrons outside a closed shell, many previous studies have shown an agreement of better than 0.5%

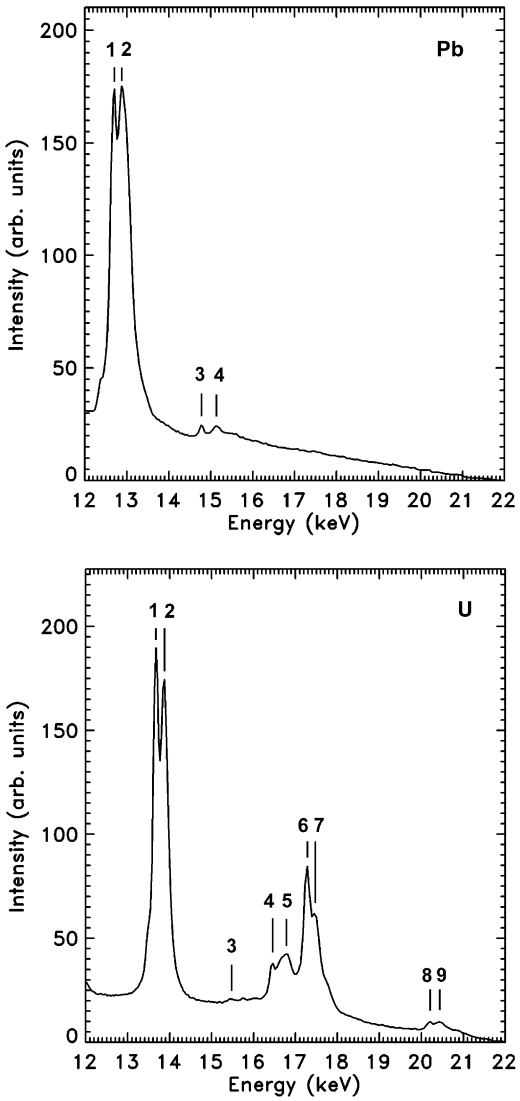

Fig. 3. The U and Pb spectra summed over the unfiltered regions of the spectral images. The line identification numbers correspond to those in Table 1.

between the measured and calculated transition energies. Therefore, we expect that the errors of the present calculated transition energies are comparable to or even smaller than the 95 eV uncertainty in the experimental energies.

A comparison of the experimental uranium spectrum with the calculated energies of the inner-shell $2l–3l'$ and $2l–4l'$ transitions in Ne-, Ar-, Ni-, Cu-, and Zn-like uranium is given in Fig. 4. The calculated intensities shown in Fig. 4 correspond to the rates for spontaneous radiative decays of these transitions. It can be seen in Fig. 4 that the calculated energies of the strongest 2p–3d transitions in Ni-like uranium are higher than the energies measured for the strongest features in the experimental

Table 1
The energies of the observed X-ray features. The designation numbers refer to Fig. 3

Designation	U energy (keV)	Pb energy (keV)
1	13.67	12.70
2	13.87	12.87
3	15.46	14.77
4	16.46	15.13
5	16.81	
6	17.28	
7	17.45	
8	20.20	
9	20.43	

Table 2
The energies of the characteristic L X-ray lines from Ref. [3]

Designation	Transition	U energy (keV)	Pb energy (keV)
α_2 $L_{III}M_{IV}$	$2p_{3/2}$–$3d_{3/2}$	13.4388	10.4495
α_1 $L_{III}M_{V}$	$2p_{3/2}$–$3d_{5/2}$	13.6147	10.5515
η $L_{II}M_{I}$	$2p_{1/2}$–$3s_{1/2}$	15.3997	11.3493
β_6 $L_{III}N_{I}$	$2p_{3/2}$–$4s_{1/2}$	15.7260	12.143
β_{15} $L_{III}N_{IV}$	$2p_{3/2}$–$4d_{3/2}$	16.3857	12.6011
β_2 $L_{III}N_{V}$	$2p_{3/2}$–$4d_{5/2}$	16.4283	12.6226
β_4 $L_{I}M_{II}$	$2s_{1/2}$–$3p_{1/2}$	16.5753	12.306
β_7 $L_{III}O_{I}$	$2p_{3/2}$–$5s_{1/2}$	16.845	12.888
β_5 $L_{III}O_{IV,V}$	$2p_{3/2}$–$5d_{5/2,3/2}$	17.0701	13.015
β_1 $L_{II}M_{IV}$	$2p_{1/2}$–$3d_{3/2}$	17.2200	12.6137
β_3 $L_{I}M_{III}$	$2s_{1/2}$–$3p_{3/2}$	17.4550	12.7933
γ_1 $L_{II}N_{IV}$	$2p_{1/2}$–$4d_{3/2}$	20.1671	14.7644
γ_2 $L_{I}N_{II}$	$2s_{1/2}$–$4p_{1/2}$	20.4847	15.101
γ_3 $L_{I}N_{III}$	$2s_{1/2}$–$4p_{3/2}$	20.7127	15.218

spectrum by ≅100 eV. The calculated energies of the corresponding transitions in Ar- and Ne-like uranium are considerably higher (≅500 and ≅800 eV, respectively) and cannot explain the observations. This suggests that inner-shell transitions in ions in the vicinity of the Ni-like sequence, but mostly in lower ionization states than Ni-like, would give the best agreement with the experimental spectrum in terms of the photon energy. It can be further seen from Fig. 4 that the transition energies in Cu- and Zn-like uranium are very similar to those of Ni-like uranium. The energy scale of Fig. 4 does not allow observation of any significant differences between the transition energies in these three ions, but in fact, there is an average of ≅20 eV separation between the transitions of the different ions. This result further narrows the candidate ions that are responsible for the bulk emission to ions that are about five times less ionized than Ni-like, i.e, around As-like. It should be noted that even though the absolute accuracy of the calculated transition energies is not expected to be 20 eV but rather ≅70 eV, the relative accuracy, i.e. with respect to the energy calculated

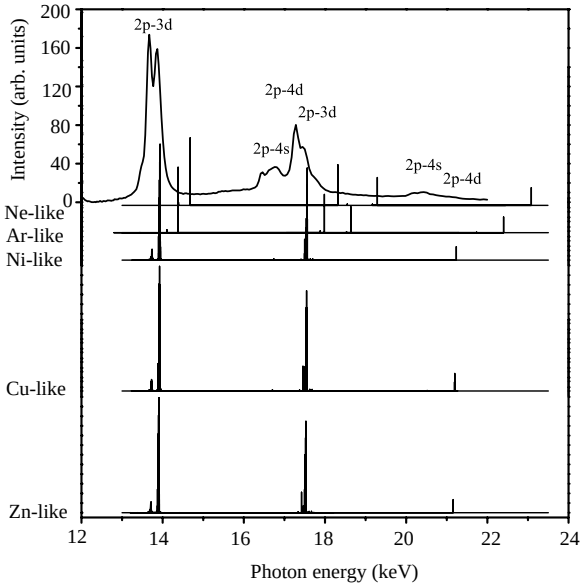

Fig. 4. Comparison of the experimental uranium spectrum and the calculated energies of L-shell transitions in the Ne-, Ar-, Ni-, Cu, and Zn-like ionization stages. The calculated intensities correspond to the rates for spontaneous radiative decays. The background continuum level was subtracted from the experimental spectrum for comparison purposes.

for the same type of transition in a different isoelectronic sequence, is much higher and sufficient to determine the trend. Unfortunately, the present version of HULLAC does not allow including a sufficient number of electronic shells necessary to perform detailed calculations of inner-shell $2l–3l'$ transitions in ionization states lower than Zn-like. However, subsequent comprehensive calculations using the averaging methods of the STA model [5–9] indeed indicate that the emission most likely results from an effective average Z of 58.3, i.e. from ions around As- and Se-like uranium.

The clearest disagreement with the experimental spectrum is the intensity ratio between the two sub-arrays within the strongest 2p–3d transition array. This disagreement is also evident when comparing the experimental spectrum with synthetic spectra generated by detailed collisional radiative models, as well as by STA simulations (assuming optically thin plasmas). We speculate that absorption effects, which were not included in the calculations, have a substantial role in forming the resultant spectra. Further theoretical and experimental studies of the opacity effect are needed in order to resolve the present disagreement in a more quantitative manner.

4. Summary

The X-ray spectra in the energy range 12–60 keV were observed from U and Pb foil targets irradiated by the OMEGA laser. Based on the energy scale established in situ by the observed absorption edges of several filters, the U and Pb spectral features appear to have energies that are higher than the characteristic (neutral atom) L-shell transitions. Calculations of the energies of L-shell

transitions in highly charged ions suggest that the observed transitions are from ionization stages lower than Ni-like and mostly around Se-like. The analysis further indicates that opacity effects might also play an important role in producing the spectra.

The identification of the observed spectral features as L-shell transitions implies that L-shell vacancies were created, most likely by energetic electrons. The binding energy of lower level of the $L\alpha_1$ transition ($2p_{3/2}$–$3d_{5/2}$) in neutral uranium is 17.166 keV. Thus, electrons with approximately this energy or higher energy are present in the plasma. By comparison, the ionization energy of Cu- and Ni-like uranium are only 4.7 and 6.9 keV, respectively.

The interpretation of the experimental spectra is that electrons with energies >17 keV create inner-shell vacancies in the U and Pb ions that are present in the plasmas. This interpretation is consistent with the observation [1] of a 22 keV K-shell line in the spectrum from a silver foil that was irradiated under the same conditions as the U and Pb foils described here. The binding energy of the neutral silver $1s_{1/2}$ level is 25.514 keV, implying that >25 keV electrons are present.

The U and Pb M-shell transitions, resulting from cascading of the L-shell transitions, are expected to appear in the 2.3–3.2 keV energy range. It will be possible to observe both the M- and L-shell transitions using the HENEX five-channel X-ray spectrometer being built for deployment at OMEGA and the National Ignition Facility [10]. This spectrometer covers the 1–20 keV energy range with 400–900 spectral resolving power. The higher resolving power of this instrument will also facilitate a more quantitative analysis of the transition energies, the identification of the ionization stages contributing to the observed spectral features, and the effect of opacity on the observed line intensities.

Acknowledgements

We thank the OMEGA laser and experimental support groups for expert technical assistance.

References

[1] Hudson LT, Henins A, Deslattes RD, Seely JF, Holland GE, Atkin R, Marlin L, Meyerhofer DD, Stoeckl C. A high-energy X-ray spectrometer diagnostic for the OMEGA laser. Rev Sci Instrum 2002;73:2270–5.

[2] Deslattes R, Kessler E, Indelicato P, Lindroth E. X-ray wavelengths. In: Wilson AJC, Prince E, editors. International tables for crystallography, vol. C. International Union of Crystallography. Dodrecht: Kluwer Academic Publishers, 1999. p. 206.

[3] Bearden JA. X-ray wavelengths. In: Weast RC, editor. CRC handbook of chemistry and physics. New York: CRC Press, 1989. p. E–151.

[4] Bar-Shalom A, Klapisch M, Oreg J. HULLAC, an integrated computer package for atomic processes in plasma. JQSRT 2001;71/2-6:169–88.

[5] Bar-Shalom A, Oreg J, Goldstein WH, Shvarts D, Zigler A. Super transition arrays—a model for the spectral analysis of hot dense plasma. Phys Rev A 1989;40:3183–93.

[6] Bar-Shalom A, Oreg J, Goldstein WH. Configuration interaction in LTE spectra of heavy elements. JQSRT 1994;51:27–39.

[7] Bar-Shalom A, Oreg J, Goldstein WH. Effect of configuration widths on the spectra of local-thermodynamic-equilibrium plasmas. Phys Rev E 1995;51:4882–90.

[8] Bar-Shalom A, Oreg J. Photoelectric effect in the super transition array model. Phys Rev E 1996;54:1850–6.
[9] Oreg J, Bar-Shalom A, Klapisch M. Operator technique for calculating superconfiguration-averaged quantities of atoms in plasmas. Phys Rev E 1997;55:5874–82.
[10] Seely J, Back C, Deslattes R, Hudson L, Holland G, Bell P, Miller M. Hard X-ray spectrometers for the National Ignition Facility. Rev Sci Instrum 2001;72:2562–5.